Iron-Starvation-Induced Mitophagy

Mediates Lifespan Extension

upon Mitochondrial Stress in *C. elegans*

Alfonso Schiavi, Silvia Maglioni, Konstantinos Palikaras, Anjumara Shaik, Flavie Strappazzon, Vanessa Brinkmann, Alessandro Torgovnick, Natascha Castelein, Sasha De Henau, Bart P. Braeckman, Francesco Cecconi, Nektarios Tavernarakis, and Natascia Ventura

Supplementary Information
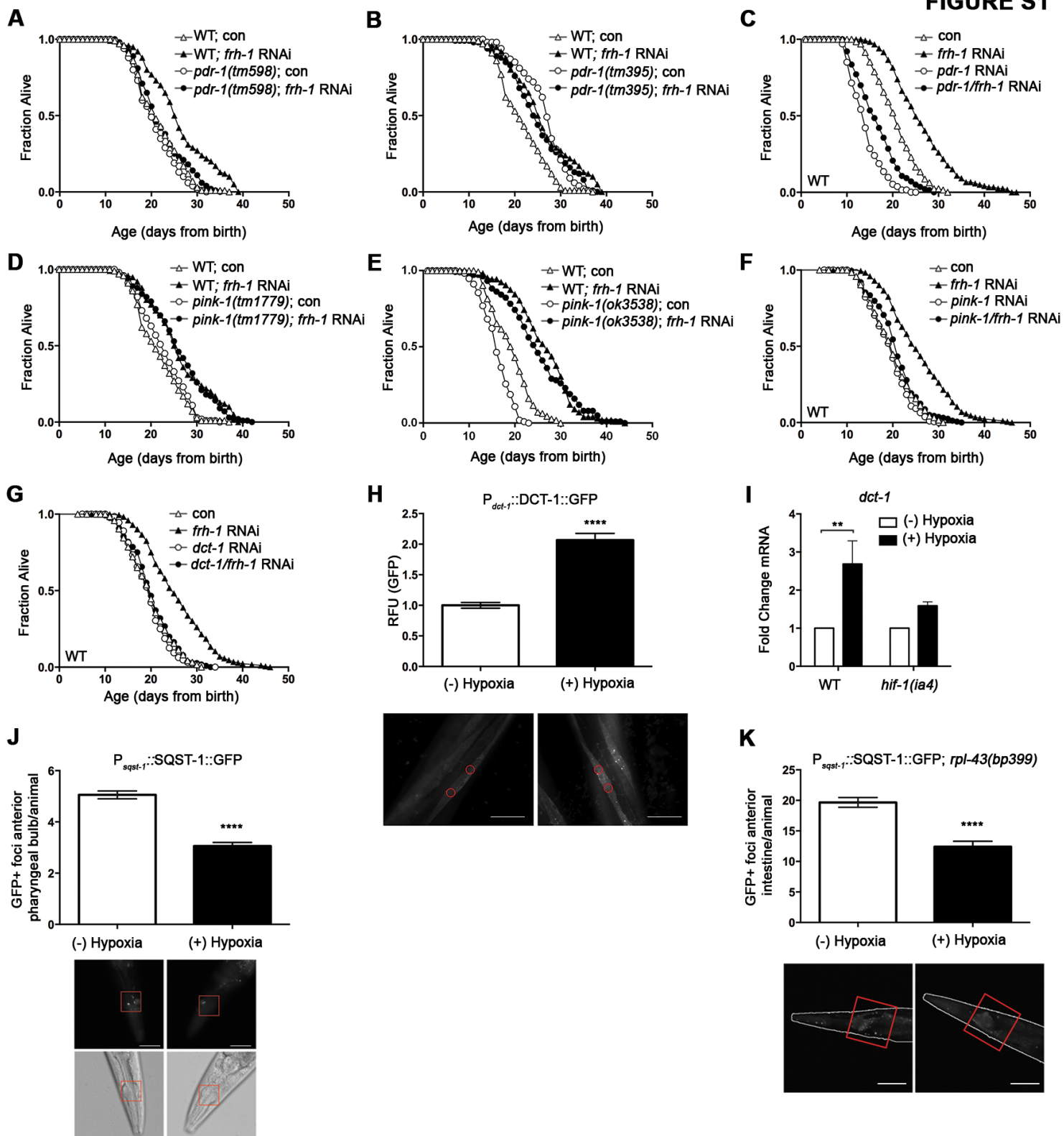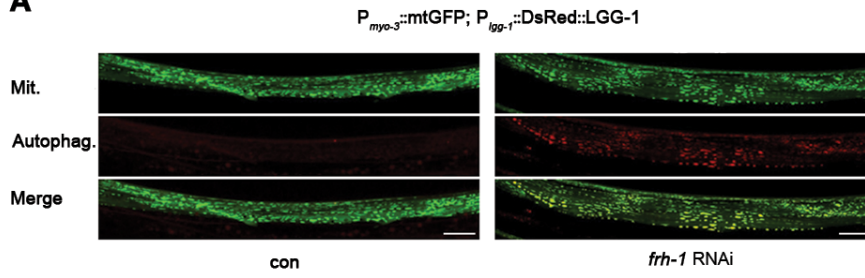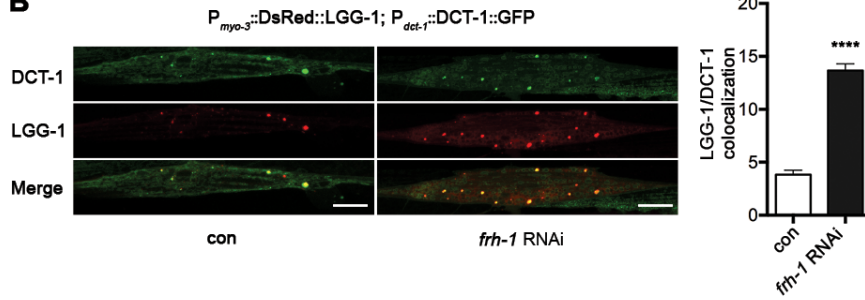
Supplemental Figures and Legends

Figure S1. Related to Figure 1. *C. elegans* **mitophagy regulatory genes mediates lifespan in response to frataxin suppression and are modulated by hypoxia.** Kaplan-Meier survival curves of wild-type (WT), *pdr-1(tm598)* **(A)**, *pdr-1(tm395)* **(B)**, *pink-1(tm1779)* **(D)**, and *pink-1(ok3538)* **(E)** strains fed bacteria transformed with either empty-vector (con) or with vector expressing dsRNA against frataxin *(frh-1)*. Kaplan-Meier survival curves of wild-type (WT) animals fed bacteria transformed with either empty-vector (con) or with vector expressing dsRNA against the indicated genes *(frh-1, pdr-1, pink-1, dct-1)* or a combination of them, *pdr-1/frh-1* RNAi **(C)** or *pink-1/frh-1* RNAi **(F)**, *dct-1/frh-1* **(G)**. **H)** Quantification of GFP intensity in the muscle of P$_{dct-1}$DCT-1::GFP transgenic strain left untreated or treated for 4 hours with hypoxia (<1% O2 at 20°C). Bottom panels show representative pictures with red circles indicating the region used to quantify the GFP. Scale bars in white are 50 μm. **I)** Quantification of *dct-1* transcript expression in wild-type (WT) and in *hif-1(ia4)* strains treated as in (H). **J)** Quantification of GFP+ foci in the anterior pharyngeal bulb of P$_{sqst-1}$SQST-1::GFP transgenic strain treated as in (H). Bottom panels show representative pictures with red squares indicating the region used to count the number of foci. Top panels: green fluorescence channel images (GFP). Bottom panels: differential (Nomarski) interference contrast images (DIC). Scale bars in white are 50 μm. **K)** Quantification of GFP+ foci in the anterior part of the intestine of P$_{sqst-1}$SQST-1::GFP; *rlp-43(bp399)* transgenic strain treated as in (H). Bottom panels show representative green fluorescence images (GFP). Highlighted with red square is the region used to count the number of foci. Scale bars in white are 50 μm. Bar graphs represent means $\pm$ SEM (n=3), ** p value < 0.01 **** p value < 0.0001.
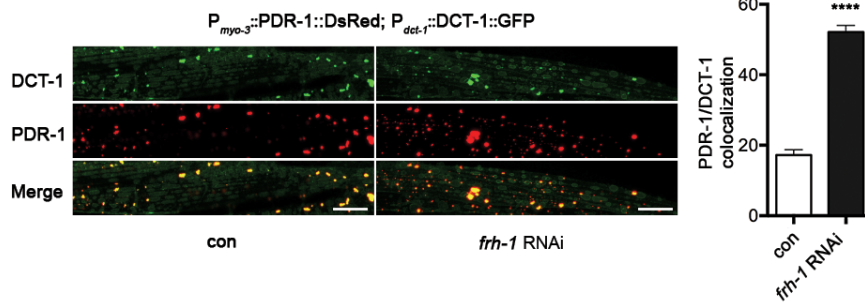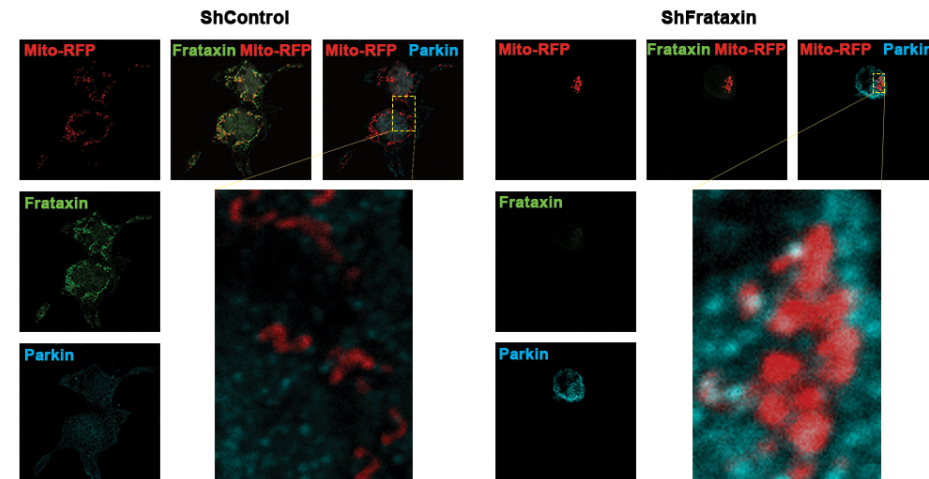
FIGURE S2

A

P*myo-3*::mtGFP; P*lgg-1*::DsRed::LGG-1

Mit.

Autophag.

Merge

con   *frh-1* RNAi

B

P*myo-3*::DsRed::LGG-1; P*dct-1*::DCT-1::GFP

DCT-1

LGG-1

Merge

con   *frh-1* RNAi

C

P*myo-3*::PDR-1::DsRed; P*dct-1*::DCT-1::GFP

DCT-1

PDR-1

Merge

con   *frh-1* RNAi

D

ShControl   ShFrataxin

Mito-RFP   Frataxin Mito-RFP   Mito-RFP Parkin   Mito-RFP   Frataxin Mito-RFP   Mito-RFP Parkin

Frataxin   Frataxin

Parkin   Parkin

E

Parkin
Actin

Total   Mitochondrial
extracts   enrichement

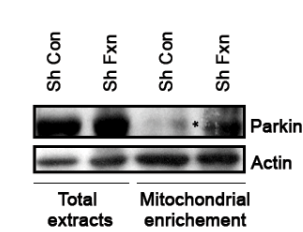**F**
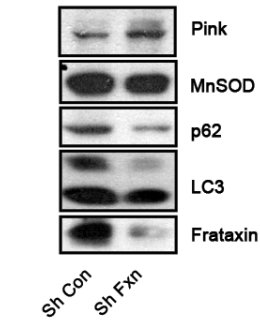
Pink
MnSOD
p62
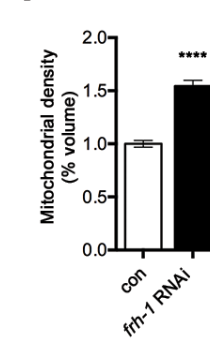LC3
Frataxin

Sh Con   Sh Fxn

G

Figure S2. Related to Figure 2. Induction of mitophagy in *C. elegans* and mammalian cells by frataxin silencing.

A) Representative confocal pictures of P_{myo-3}::mtGFP;P_{lgg-1}::DsRed::LGG-1 transgenic strain fed bacteria transformed with either empty-vector (con) or vector expressing dsRNA against *frh-1* (*frh-1* RNAi). In green muscle mitochondria (Mit), in red the Autophagosomes (Autopag.), in yellow the overlapping between the two (Merge). Scale bars indicate 20μm. **B)** Quantification of the colocalization between autophagosomes and DCT-1 in P_{myo-3}::DsRed::LGG-1; P_{dct-1}::DCT-1::GFP transgenic animals fed as in (A). Left panels show representative confocal picture of *C. elegans* muscles acquired using a 40X objective lens: in green DCT-1, in red the autophagosomes (LGG-1), in yellow the overlapping between the two (Merge). Scale bars indicate 20μm. **C)** Quantification of the colocalization between PDR-1 and DCT-1 in P_{myo-3}::PDR-1::DsRed; P_{dct-1}::DCT-1::GFP transgenic animals fed as in (A). Left panels show a representative confocal picture of *C. elegans* muscles acquired using a 40X objective lens: in green DCT-1, in red PDR-1, in yellow the overlapping between the two (Merge). Scale bars indicate 20μm. **D)** Representative confocal images of HEK293 cells transiently transfected with ShControl or ShFrataxin showing typical features of mitophagy induction upon frataxin silencing: parkin translocation to mitochondria (see enlarged inset from Mito-RFP and Parkin overlaid images) and perinuclear redistribution of mitochondria. Mitochondria are stained in red, nuclei with DAPI (shown in grey), Frataxin in revealed in green with secondary anti-Mouse Alex Fluor 488, while Parkin is reveled in cyan using a secondary antibody anti-Rabbit Alexa Fluor 647. **E)** Representative western blot using anti-Parkin and anti-Actin as loading control from total extract and enriched mitochondrial fraction from HEK293 cells transiently transfected with an empty vector (Sh Con) or a vector encoding ShRNA against Frataxin (Sh Fxn). * Parking specific band. **F)** Representative western blot using the indicated antibodies on enriched mitochondrial fraction (MnSOD was used as loading control to quantify Pink-1 increase shown in Figure 2) from HEK293 cells transiently transfected with an empty vector (Sh Con) or a vector encoding ShRNA against Frataxin (Sh Fxn). **G)** Quantification of mitochondrial density expressed as percentage of mitochondrial volume in the total analysed volume normalized to the control from P_{rps-0}::*gas-1*::DENDRA2 transgenic worms fed bacteria transformed with empty-vector (con) or with vector expressing dsRNA against *frh-1* (*frh-1* RNAi). Bars graph represent means ± SEM (n=3), **** p value < 0.0001.
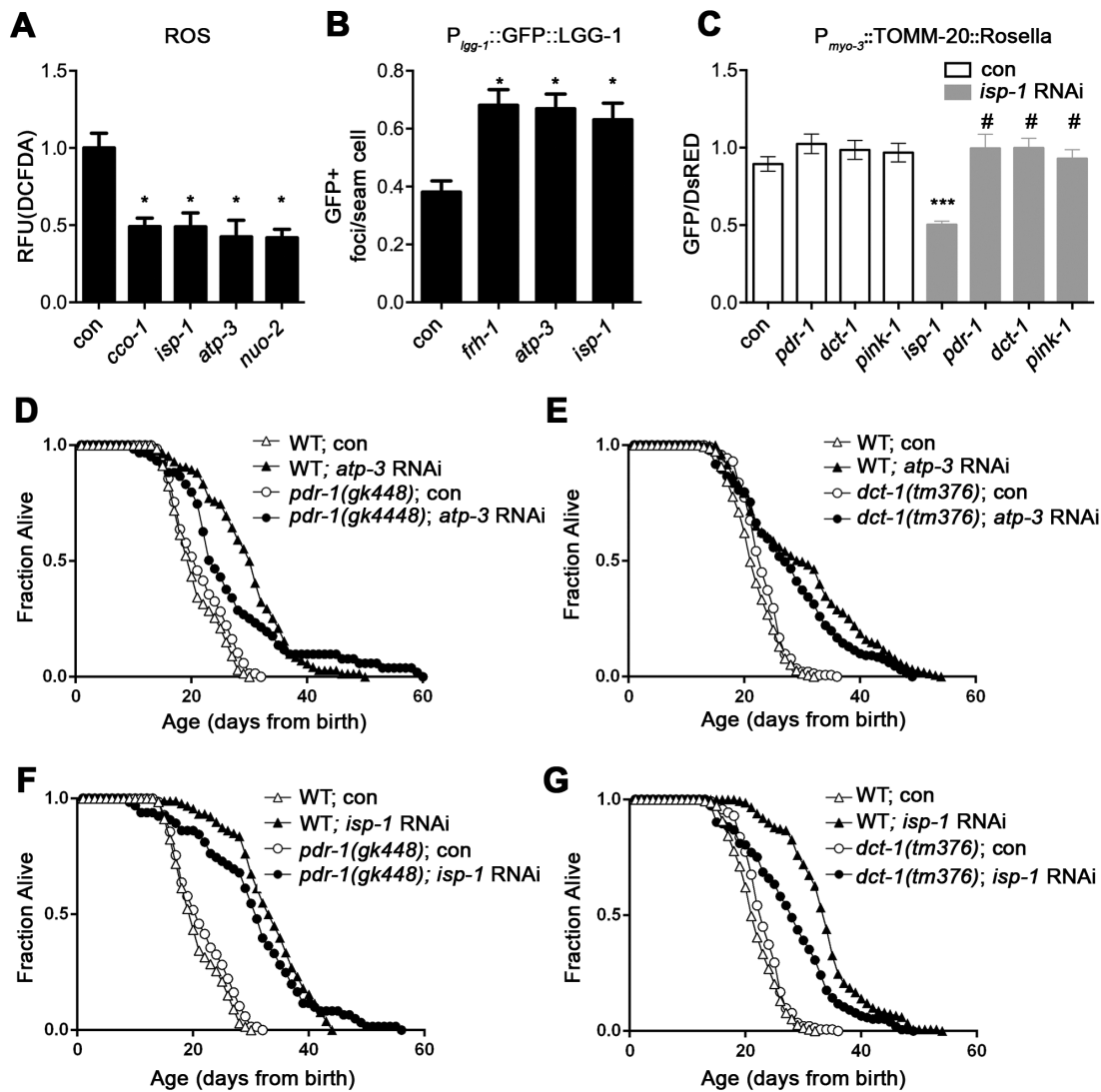
Figure S3. **Related to Figures 1 and 2. Mitophagy mediates lifespan extension in response to mitochondrial stress.** **A)** Quantification of reactive oxygen species (ROS) content (H2-DCFDA) from extract of 1-day-old wild-type animals fed bacteria transformed either with empty-vector (con) or with vector expressing dsRNA against the indicated genes. RFU = Relative Fluorescence Unit. **B)** Quantification of GFP+ foci in the seam cells of P_{lgg-1}::GFP::LGG-1 transgenic strain fed bacteria transformed either with empty-vector (con) or with vector expressing dsRNA against the indicated genes. **C)** Mitochondrial autophagy was quantified using the ratio between green and red fluorescence (GFP/DsRED) in P_{myo-3}::TOMM-20::Rosella transgenic animals fed bacteria transformed either with empty-vector (con) or with vector expressing the indicated dsRNA. Bar graphs represent means ± SEM (n=3). **D-G)** Kaplan-Meier survival curves of wild-type (WT), *pdr-1(gk448)* or *dct-1(tm376)* mutants fed bacteria transformed with empty-vector (con) or with vector expressing dsRNA against *atp-3* or *isp-1*. Bar graphs represent means ± SEM (n=3), * p value < 0.05, *** p value < 0.001, # p value <0.0001.
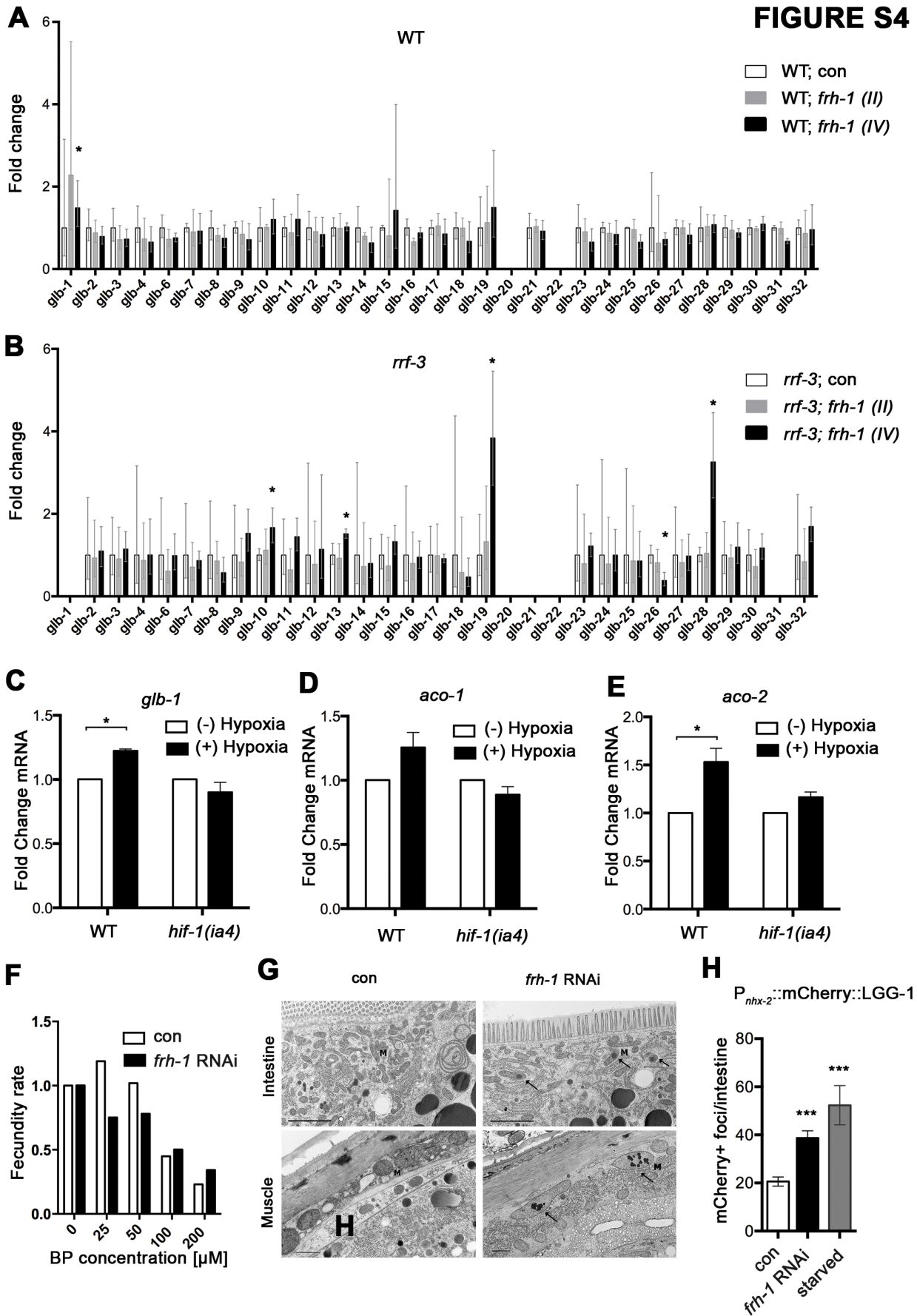
Figure S4. Related to Figure 3 and 4. Frataxin silencing induces a hypoxia-like, iron starvation response. A, B) Transcript levels of *C. elegans* globin genes (*glb1*−*glb-33*) were measured by qRT-PCR **A)** in wild-type animal (WT) or **B)** in the RNAi hypersensitive mutants *rrf-3(pk1426) (rrf-3)* [S1], which displayed enhanced sensitivity to *frh-1* RNAi [S2]. Animals in A) and B) were fed bacteria transformed either with empty-vector (con) or with vector

expressing dsRNA against *frh-1* (*frh-1* (IV)) or a *frh-1 dsRNA* (*frh-1 (II)*) that does not extend longevity [S3]. Bars and errors represent genes mean expression and its 95% confidence interval **C-E)** Quantification of *glb-1, aco-1* and *aco-2* transcripts expression in wild-type and *hif-1(ia4)* strains left untreated or treated for 4 hours with hypoxia (<1% O2 at 20°C). Bars and errors represent means ± SEM (n=3). **F)** Number of eggs laid per worm per hour (fecundity rate) was quantified in wild-type animals fed bacteria transformed either with empty-vector (con) or with vector expressing dsRNA against *frh-1* (*frh-1* RNAi*) after L4 larvae were left untreated or treated for 24 hours with the indicated concentrations of the iron chelator BP. The number of laid eggs was normalized against the number of eggs laid in untreated animals. G) Electron micrographs of young adult wild-type worms fed as in (F). Size bars = 1μm. Electron-dense inclusions (arrows) accumulate in muscle and intestine mitochondria (M) only in *frh-1* RNAi treated animals. H) Quantification of mCherry+ foci in the intestinal cells of young adults P$_{nhx-2}$::mCherry::LGG-1 transgenic strain fed as in (A) or starved overnight before quantification. Bar graphs represent means ± SEM (n=3), * p value < 0.05, *** p value < 0.001.

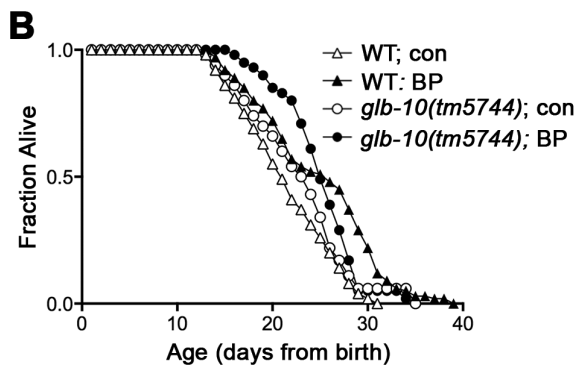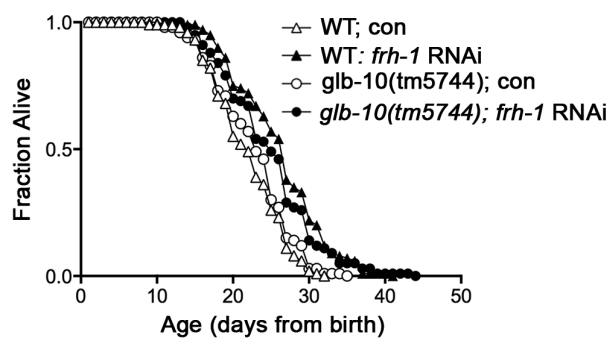**Figure S5. Related to Figure 6. Frataxin and iron depletion act through independent pathways. A, B)** Kaplan-Meier survival curves of wild-type animals (WT) and *glb-10(tm5774)* fed bacteria transformed with empty-vector (con) or with vector expressing dsRNA against *frh-1* (*frh-1* RNAi) (**A**) or left untreated or treated from eggs with 10μM of BP (**B**).

Tables

Table S1. Summary of lifespan analysis.

	Genotype	RNAi	Mean Lifespan	SEM	p vs con	p vs N2	Sample size	Censor
FIG. 1	Wild-type (N2)	con	19.0	0.3			370	45
		frh-1	25.5	0.4	<0.0001		290	79
	pdr-1(gk448)	con	20.8	0.3		<0.0001	370	29
		frh-1	22.5	0.5	<0.0001	0.0001	292	107
	Wild-type (N2)	con	20.2	0.3			240	16
		frh-1	27.9	0.5	<0.0001		240	81
	dct-1(tm376)	con	22.3	0.3		<0.0001	240	25
		frh-1	25.1	0.4	<0.0001	<0.0001	240	80
	Wild-type (N2)	con	19.3	0.4			150	22
		frh-1	26.0	0.6	<0.0001		150	43
	sqst-1(ok2869)	con	21.4	0.4		0.0016	150	19
		frh-1	21.3	0.5	0.8	<0.0001	150	47
FIG. 3	Wild-type (N2)	con	20.5	0.3			320	13
		frh-1	25.9	0.5	<0.0001		317	89
	hif-1(ia4)	con	24.0	0.5			150	46
		frh-1	22.6	0.6	0.1823	0.3783	147	40
	vhl-1(ok161)	con	23.4	0.6		<0.0001	160	18
		frh-1	22.5	0.5	0.0503	<0.0001	160	40
	Wild-type (N2)	con	20.0	0.4			210	24
		frh-1	25.9	0.5	<0.0001		210	38
		aha-1	19.9	0.3	0.6353		208	27
		aha-1/frh-1	19.1	0.4	0.5385	0.8358@	210	62
FIG. 4	Wild-type (N2)	con	19.0	0.4			273	33
		frh-1	22.7	0.5	<0.0001		280	37
		con; FAC	15.7	0.3	<0.0001		266	25
		frh-1; FAC	21.0	0.3	<0.0001#	<0.0001*	268	38
	Wild-type (N2)	con	20.3	0.4			160	43
		frh-1	23.4	0.6	<0.0001		157	49
		con; BP	21.9	0.5	0.0109		157	35
		frh-1; BP	24.6	0.6	0.1757#	0.0001*	161	53
	Wild-type (N2)	con	20.1	0.4			160	12
		frh-1	23.2	0.4	<0.0001		160	57
	smf-3(ok1035)	con	25.1	0.4		<0.0001	160	25
		frh-1	24.6	0.5	0.7406	0.0293	160	30
FIG. 5	Wild-type(N2)	con	20.2	0.5			160	14
		BP	24.0	0.5	<0.0001		160	23
	dct-1(tm376)	con	22.3	0.5		0.0019	160	12
		BP	23.9	0.5	0.0275	0.8708	160	27
	pdr-1(gk448)	con	22.9	0.4		0.0005	160	5
		BP	25.6	0.6	<0.0001	0.0181	160	17
	Wild-type(N2)	con	19.3	0.4			150	22
		BP	21.9	0.6	<0.0001		150	25
	sqst-1(ok2869)	con	21.4	0.4		0.0016	150	19
		BP	22.2	0.4	0.2542	0.9444	150	12
FIG. 6	Wild-type(N2)	con	20.4	0.4			240	43
		BP	22.4	0.4	0.0014		237	35
	hif-1(ia4)	con	24.6	0.5		<0.0001	230	46
		BP	26.5	0.5	0.0031	<0.0001	238	37
	Wild-type(N2)	con	20.2	0.5			160	14
		BP	24.0	0.5	<0.0001		160	23
		frh-1	26.2	0.6	<0.0001		160	48
	egl-9(sa307)	con	27.7	0.7		<0.0001	160	100 (90)^
		BP	26.4	0.7	0.2845	0.0009	160	80 (72)^
		frh-1	33.6	0.7	<0.0001	<0.0001	160	45 (33)^
	Wild-type(N2)	con	20.0	0.4			150	22
		BP	22.3	0.5	0.0003		150	27
	glb-10(tm5533)	con	19.6	0.4		0.3732	150	35
		BP	22.9	0.5	<0.0001	0.4101	150	46
	Wild-type(N2)	con	19.7	0.4			150	24
		frh-1	22.4	0.5	<0.0001		150	54
	glb-10(tm5533)	con	20.5	0.5		0.1248	150	46
		frh-1	20.5	0.5	0.9198	0.0119	150	54

	Genotype	RNAi	Mean Lifespan	SEM	p vs con	p vs N2	Sample size	Censor
FIG. S1	Wild-type (N2)	con	21.7	0.5			135	21
		frh-1	26.3	0.7	<0.0001		135	36
	pdr-1(tm598)	con	20.8	0.5		0.1377	135	30
		frh-1	22.3	0.5	0.0145	<0.0001	135	31
	pdr-1(tm395)	con	26.6	0.5		<0.0001	135	17
		frh-1	25.0	0.7	0.6885	0.0847	135	57
	pink-1(tm1799)	con	22.7	0.5		0.1833	135	20
		frh-1	26.1	0.7	<0.0001	0.6529	135	31
	Wild-type (N2)	con	20.0	0.4			210	24
		frh-1	25.9	0.5	<0.0001		210	38
		pdr-1	13.2	0.3	<0.0001		140	7
		pdr-1/frh-1	15.7	0.4	<0.0001	<0.0001@	140	0
		pink-1	19.4	0.3	0.0905		208	23
		pink-1/frh-1	20.9	0.4	0.1043	0.0021@	210	48
		dct-1	19.2	0.4	0.1016		140	12
		dct-1/frh-1	20.4	0.5	0.5139	0.0421@	140	24
	Wild-type (N2)	con	17.9	0.3			210	25
		frh-1	24.6	0.6	<0.0001		130	31
	pink-1(ok3538)	con	14.7	0.3		<0.0001	210	62
		frh-1	23.3	0.7	<0.0001	0.6259	130	30
FIG. S3	Wild-type(N2)	con	17.9	0.3			210	31
		isp-1	31.3	0.7	<0.0001		110	30
		atp-3	27.7	0.8	<0.0001		103	27
	pdr-1(gk448)	con	19.0	0.4		0.0068	210	24
		atp-3	28.7	1.2	<0.0001	0.0001	103	45
		isp-1	25.0	1.4	<0.0001	0.4072	91	35
	Wild-type(N2)	con	20.2	0.3			240	16
		isp-1	32.8	0.5	<0.0001		160	10
		atp-3	29.4	0.8	<0.0001		159	4
	dct-1(tm376)	con	22.3	0.4		<0.0001	240	25
		isp-1	27.1	0.7	<0.0001	<0.0001	160	7
		atp-3	27.1	0.8	<0.0001	0.0205	160	28
FIG. S5	Wild-type (N2)	con	21.0	0.5			135	26
		frh-1	25.2	0.6	<0.0001		135	38
	glb-10(tm5744)	con	21.7	0.5		0.1551	135	41
		frh-1	24.0	0.7	0,0041	0.2860	135	49
	Wild-type (N2)	con	20.5	0.7			70	19
		BP	23.9	0.8	<0.0001		70	5
	glb-10(tm5744)	con	21.8	0.8		0.2191	70	33
		BP	24.2	0.6	0.08	0.2161	70	29

Table S1. Each set of lifespan analysis is associated with its corresponding figure in the text as indicated on the left of the table. Means, standard deviation of the mean (SEM) and P values were calculated using the log-rank test (Mantel-Cox) from Kaplan-Meier survival analysis of cumulative data obtained from the indicated numbers of animals.

p value vs *frh-1;* * p value vs treated control; @ p value vs single RNAi without *frh-1;* ^ in parenthesis is the number of animals censored because of internal bagging in the *egl-9* mutants, where this phenotype has been originally ascribed to an egg-laying deficit [S4].

Supplemental Experimental Procedures

Mammalian Cells

Cell line and transfection

The human embryonic kidney HEK293 cells were cultured in Dulbecco's modified Eagle's medium (DMEM, Sigma-Aldrich) supplemented with 10% FCS, 2 mM l-glutamine, and 1% penicillin/streptomycin. Transient transfections of expression plasmids Sh-scramble and Sh-Frataxin (kindly provided by Dr. Testi laboratory [S5]) were performed using TurboFect Transfection Reagent (Thermo Scientific).

Cell extracts

HEK293 cells were lysed in RIPA buffer (150 mM NaCl, 50 mM Tris pH 7.4, 1% Triton, 0,5% Nonidet P40, 10% glycerol, 2.5% sodium deoxycholate) plus protease and phosphatase inhibitors. Protein concentrations were determined with the Biorad Protein Assay. Cell extracts were separated by SDS-PAGE and transferred onto nylon membranes (Immobilon P, Millipore, Bedford, MA). Mitochondria were enriched from HEK293 cells by standard differential centrifugation method and suspended in isolation buffer (IB; 0.2 M sucrose, 10 mM Tris-MOPS [pH 7.4], 0.1 mM EGTA-Tris, 0.1% delipidated BSA).

Western blot analysis

Cell extracts were separated by SDS-PAGE and transferred onto nylon membranes (Immobilon P, Millipore, Bedford, MA). Membranes were incubated with primary antibodies followed by horseradish peroxidase-conjugate secondary antibody (Jackson Laboratory) and visualized with ECL plus (Amersham Bioscience). Primary antibodies: polyclonal anti-PINK (Novus Biologicals, BC100-494), polyclonal anti-PARKIN (Santa Cruz, H-300- sc-30130), mouse monoclonal anti-ACTIN (Sigma–Aldrich), polyclonal anti-MnSOD (Assay Designs), polyclonal anti-LC3 (Cell signaling), monoclonal anti-p62 (Santa-Cruza, sc-28359) and monoclonal anti-Frataxin (MAB-10876, Immunological Sciences)

Immunocytochemistry

Cells were washed in PBS and fixed with 4% paraformaldehyde in PBS for 15 min. After permeabilization with 0.4% Triton X-100 in PBS for 5 min, cells were blocked in 3% Normal goat serum in PBS and incubated over-night at 4 degrees with primary antibodies. We used the antibodies directed against PARKIN and Frataxin. Cells were then washed in blocking buffer and incubated for 1 h with labelled anti-mouse (Alexa Fluor 488 or Alexa Fluor 555, Molecular Probes, Eugene, OR) or anti-rabbit (FITC or Cy3, Jackson ImmunoResearch, West Grove, PA) secondary antibodies. Nuclei were stained with 1 µg/ml DAPI and stained cells were then examined through confocal laser scanning microscopy (Zeiss LSM 700) 100x oil-immersion objective. We used "ZEN 2009 Light edition" software for image analysis.

Caenorhabditis elegans

Nematode strains used in this work.

Standard conditions for *C. elegans* strains culture and RNAi experiments were used [S6-7]. Strains used in this work are:

N2:wild-type (Bristol), ZG31:*hif-1(ia4)*, *dct-1(tm376),* VC2149:*sqst-1(ok2869),*

PP2035:*rpl-43*(*bp399*)II; bpIs151[P*sqst-1*::SQST-1::GFP; unc-76(+)],

PP1545:bpIs151[P*sqst-1*::SQST-1::GFP; unc-76(+)]IV; *him-5*(*e1490*)V, BC12921:P*sqst-1*::GFP; dpy-*5(e907)* I, VK1093:*vkEx1093*[P*nhx-2::mCherry::lgg-*1], NV25:*adIs2122*[P*lgg-1*::GFP::*lgg-1*;pRF4+], NV27:*adIs2122*[P*lgg-1*::GFP::*lgg-1*;pRF4+]; *hif-1(ia4)*, JT307:*egl-9(sa307)*, CB5602:*vhl-1(ok161),* ZG120:*iaIs07*[P*nhr-57*::GFP;*unc119*+], ZG175:*iaIs07*[P*nhr-57*::GFP;*unc119*+]; *hif-1(ia04)*, NL2099:*rrf-3(pk1426),* FX05744:*glb-10(tm5744),* FX05533:*glb-10(tm5533),* P*glb-10*::GFP; P*glb-19*::GFP, P*glb-28*::GFP, P*glb-26*::*glb-26*::GFP, XA6901: *lin-15(n765ts)*; *qaEx2* [*ftn-2*::Dpes-10::GFP-his; *lin-15+*], N2*; Ex*[P*myo-3*::TOMM-20::Rosella], N2*; Is*[P*myo-3*::mtGFP]*; Ex[P*lgg-1*::DsRed::*lgg-1*], N2*; Ex*[p*myo-3*PDR::DsRed;p*dct-1*DCT::GFP], N2*; Ex*[p*myo-3*DsRed::LGG-1; p *dct-1*DCT::GFP].

VC1024:*pdr-1(gk448)* carries a 372bp deletion that removes the 5'UTR and part of the coding sequence leading to undetectable gene transcript [S8]. FX00598:*pdr-1(tm598)* and

FX00395:*pdr-1(tm395)* carry an in-frame 697bp deletion and an out-of-frame 480bp deletion respectively [S9]. *pink-1(tm1779)* carries a 350bp null-mutation [S10] while RB2547:*pink-1(ok3538)* carries a 500bp deletion (http://www.cgc.cbs.umn.edu/strain.php?id=16867).

Lifespan analysis

Survival analysis started from hatching and were scored at 20°C using synchronous populations of 70-100 animals per strain. Animals were scored as dead or alive and transferred every day on fresh RNAi plates during the fertile period, and then every other day or every 3 days until death. Worms were considered dead when they stop pharyngeal pumping and responding to touch. Worms that die because of internal bagging, desiccation due to crawling on the edge of the plates, or gonad extrusion were scored as censored and included in the statistical analysis. Exposure to 6.6mg/ml Ammonium iron (III) Citrate, FAC (Sigma, cat#F5879-100GR) [S11] and to 10μM 2,2 dipyridyl, BP (Carl Roth, cat#4153.2), was performed supplementing the NGM medium.

Quantification of GFP-transgene expression by automated fluorescence microscopy

Sixty transgenic adult stage worms were transferred to 96-well plates containing 270μl of S-Basal and anesthetized with 2μl of 1M NaN_3 (Sigma, cat#S2002-25G) prior to image capture. NaN_3 treatment prevents z-axis movements ensuring animals are in a uniform plane for imaging. Images were acquired with the ArrayScan V^{TI} HCS Reader (Cellomics, ThermoFisher) fitted with a 1.25× objective and a 0.63× coupler. For the detection of worms and quantification of the expression of fluorescent signal, images were captured using the SpotDetector BioApplication. For image capture and following analysis of the lines expressing fluorescent transgenes, we employed a 2-channel (brightfield and GFP) assay. Algorithms were optimized to first identify valid objects (in a optimal population size), defined as non-overlapping, whole worms in the brightfield channel. Debris and partial worms were automatically excluded from analysis. Fluorescent transgene expression, within valid objects, was quantified in the GFP channel. SpotDetector BioApplication parameters were optimized to identify transgene expression as spots of different shape, size and intensity. Specifically, object

count, spot count and spot total intensity per object were used to compare GFP expression in different transgenic strains: for P*ftn-2*::GFP and P*glb-26::glb-26*::GFP, with a punctate GFP expression pattern, the signal was calculated as average spot intensity; for P*glb-19*::GFP, P*glb-28*::GFP and P*nhr-57*::GFP, with a diffuse GFP expression pattern the signal was calculated as total average intensity.

Quantification of GFP-transgene expression by fluorescence microscopy

The effect of frataxin silencing, iron chelation or hypoxia on the induction of different transgenic strains was investigated on synchronized population of adult worms. The nematodes were placed in a 14 μl S-Basal drop on a microscope glass slide, anesthetized with NaN_3 10mM, covered with a cover slide and immediately imaged. Pictures were acquired with an Imager2 Zeiss fluorescence microscope, magnification 10-fold. The images were analyzed with the software ImageJ (http://imagej.nih.gov/ij/). The intensity of the GFP signal in the ZG120 and ZG175 strains was quantified considering three circular spots of the same area in each animal (head, middle body and tail). A minimum of 15 to 20 animals per condition were acquired. The graph represents the mean and the SEM of three independent biological replicates. In the PP2035 strain the same area was selected in each animal from the anterior intestine and used to count the number of GPF+ foci. 10 to 20 animals per condition were acquired. The plot represents the mean and the SD of one experiment. In the PP1545 the number of foci was quantified in the same selected area in the anterior pharyngeal bulb of each animal [S12]. A minimum of 25 animals per condition were acquired. The plot represents the mean and the SEM of at least three independent biological replicates. For quantification of the GFP P*dct-1*::DCT-1::GFP strain the same area was selected in 2 different points of a single muscle in each animal and used to quantify the relative fluorescence signal. A minimum of 20 animals per condition were acquired. The plot represents the mean and the SEM of at least three independent biological replicates.

Quantitative Real Time PCR

Routine methods for mRNA purification and cDNA synthesis were carried out as previously described [S13]. For quantification of *aco-1, aco-2* and *dct-1* transcripts, genes primer pairs were designed with Primer Blast (http://www.ncbi.nlm.nih.gov/tools/primer-blast/) and purchased from SIGMA; gene expression was quantified and normalized (using two housekeeper, *pmp-3* and F23B2.13) utilizing the Biorad iQTM5 multi color real time PCR detection system with the SyBrGreen PCR Master Mix, and the 2-ΔΔCt method. Globin genes were instead quantified with primer pairs designed as described in detail [S14]. The expression of globin genes was quantified using a Rotor-Gene 2000 centrifugal real-time cycler (Corbett Research) with the Platinum SyBrGreen qPCR SuperMix-UDG (Invitrogen, cat#11733038) as previously described [S15]. The threshold cycle (Ct) values of the Rotor-Gene software version 6.0 (Corbett Research) were exported to qBase version 1.3.5 [S16] for further analysis. For each primer set, reaction efficiency estimates were derived from standard curves that were generated using serial dilutions of a cDNA pool of all nematode samples. These were then used by qBase to transform the Ct values to relative quantities, which were normalized using the geometric mean of three reference genes identified by the geNorm 3.4 software [S17]. Next, the normalized expression levels were converted into logarithmic values to calculate the mean expression per nematode sample and its 95% confidence interval [S18]. Finally, all values were linearized again using a power function. Regardless of primer pairs design and quantification methods, a single melting peak for each reaction confirmed the identity of each PCR product with every primer pair. All assay included a no-template control for every primer pair and all measurements were produced in triplicate. Primers sequence can be provided upon request.

Electron microscopy

First-day gravid adults from synchronized populations of about ~1000 animals were mixed with a thick pellet of *E.coli*, loaded into type B high pressure freezing planchettes (Baltec) and immediately frozen in the Wohlwend Compact-02 high-pressure freezer (4 blocks for each sample). Samples were transferred to vials containing 2% Osmium tetroxide and 0.05% Uranyl acetate in 100% acetone where they were maintained for 4 days at -80°C while freeze

substitution occurred. After slowly warming to room temperature over 48 hours the samples were rinsed in 100% acetone and infiltrated with Araldite/Embed-812 (EMS), and polymerized. Thin sections (an average of 6 sections at varying depth per worm) were stained with 2% Uranyl acetate and Reynold's lead citrate and imaged at 80 kV on a Phillips CM10 electron microscope. Images were acquired only when representative tissues and mitochondria in well-preserved samples were found. Shown are representative pictures from 2 experiments were images were taken from 5 worms per samples. No quantification was done since none of the wild-type animals displayed dark electron-dense granule while all sections analyzed from *frh-1* RNAi animals display dark deposits in at least one mitochondrion.

Iron chelation sensitivity

For iron depletion sensitivity assays the iron chelator 2,2′-dipyridyl, BP (Carl Roth, cat#4153.2) was supplemented to NGM in concentrations of 25μM, 50μM, 100μM and 200μM. The effect of BP on animal development was investigated on synchronized worms fed with *E. coli* HT115 expressing the control vector L4440 or *frh-1* dsRNA for three generations. A population of eggs was laid on control and BP plates and the number of eggs was counted. After 3 days, 4 days and 5 days from the egg lay the number of laid eggs hatched and developed into gravid adults was calculated. To test the effect of BP on the fertility, semi-synchronized L4 larvae (fed as above) were instead transferred to BP plates for 24 hours and grown to gravid adults. Three worms from each condition were then transferred to regular NGM plates without BP and fecundity (number of eggs laid) and fertility rates (fraction of eggs hatched) were calculated. The relative fecundity was normalized to the mean values of non-treated animals. To assess the expression of transgenes in response to iron chelation, synchronized larvae were grown for 24 h on NGM plates then transferred as L4 larvae to NGM plates supplemented with 100μM BP for 18 h before GFP expression quantification.

ROS content

For ROS measurements populations of ~1000 synchronized young adult animals were collected in S-basal, washed and immediately lysed in 300μl of S-Basal plus protease inhibitor cocktail

(Sigma, cat#P2714) subjected to sonication. Reactive oxygen species were quantified utilizing 50μg of extract incubated in 500μl of a 5mM H2-DCF-DA (2-7-dichlorofluorescein-diacetate) (Sigma, cat#D6883-50MG) solution in S-Basal plus protease inhibitor cocktail. Each sample was read in triplicate (150μl each) in flat bottom 96-well plate in a Wallac 1420 Victor microplate reader at excitation/emission wavelengths of 485 and 528 nm. Different readings were carried out over a time frame of 2 hours to control that reaction was occurring properly.

Autophagy measurements

The number of autophagic GFP positive foci was counted in the seam cells of *Plgg-1::*GFP*::*LGG-1 [S3] L3 larvae mounted on 2% agarose pads using 100-fold magnification on a Zeiss Axio Imager2 microscope. At least three independent biological trials were carried out and the mean ± SEM number of foci in maximum 8 seam cells per worm from at least 10 worms was plotted from each condition. mCHERRY positive foci from the P*nhx-2::mCherry::*LGG-1 [S19] transgenic strain were counted in the intestine of young adults worms. At least three independent biological trials were carried out and the number of foci from 10 to 15 animals was plotted as mean ± SEM. To quantify p62::GFP puncta, the number of GFP foci was quantified in the anterior pharyngeal bulb of the *Psqst-1:*SQST-1::GFP [S12] transgenic strain (see above). Worms were mounted on agarose pads and pictures were acquired using 100-fold magnification on a Zeiss Axio Imager2 microscope. Due to intense background fluorescence in mCherry::LGG-1 and p62::GFP strains, the background was substracted using ImageJ (http://imagej.nih.gov/ij/) and foci were counted manually on the adjusted images.

Mitophagy measurement

To monitor mitophagy process four newly developed *C. elegans* strains were used: N2*;Is*[p$_{myo-3}$mtGFP]*;Ex[*p$_{lgg-1}$DsRed::LGG-1], N2*;Ex*[p$_{myo-3}$PDR-1::DsRed;p$_{dct-1}$DCT-1::GFP], N2*;Ex*[p$_{myo-3}$DsRed::LGG-1;p $_{dct-1}$DCT-1::GFP], N2*;Ex*[p$_{myo-3}$TOMM-20::Rosella] [S20]. The first three strains allowed the visualization of the colocalization between mitochondria and the autophagosomes during mitophagy induction through confocal microscopy. The latter, thanks

to the dual-emission fluorescence pH-biosensor targeted to mitochondria, allowed the assessment of mitochondrial delivery to the lysosomes during mitochondrial autophagy.

L4 transgenic larvae were grown on either the control (pL4440) vector or *frh-1* RNAi plates. Images were acquired using a 40x or 100x objective lens using the Zeiss LSM 710 confocal microscope. Mitophagy induction is revealed as colocalization between green and red fluorescence. More then 50 body wall cells per assay were counted. Three independent biological trials were carried out and representative images are shown in the figures.

Transgenic animals expressing TOMM-20::Rosella biosensor in body-wall muscle mitochondria cells were examined under a Zeiss AxioImager Z2 epifluorescence microscope. The fluorescent pH-biosensor, Rosella [S21-22] targeted to mitochondria allow to follow their delivery into the lysosomes for degradation. The assay relies on the dual emission of a tandem tag consisting of a pH-stable DsRed and a pH-sensitive GFP variant. In normal conditions mitochondria fluorescence both red and green, while upon induction of mitochondrial autophagy, the delivery of mitochondria into the acidic lysosome compartment mainly quenches the green but not the red fluorescence leading to a reduced GFP/dsRed ratio. L4 larvae were grown on either the control (pL4440) vector or the test RNAi plates with or without the presence of the iron chelator 2,2-dipyridyl (BP). Three independent biological trials of each condition were carried out and the mean and SEM of pixel intensity was averaged and plotted.

Mitochondrial Density

Dendra2 transgenic worms (*rps-0p::gas-1*::DENDRA2 [S23]) at day two of adulthood were immobilized on 2.5% agarose pads using 5 mM levamisole (Sigma). A Nikon TiE-C2 confocal laser scanning microscope was used for optical imaging. Z-stacks (68 images, 256×256 pixels, 15 μm total depth) of the posterior half of the worm were collected by exciting with a 488-nm solid state laser, scanned with a 60× Plan Apochromat objective (NA 1.20, water immersion) and detected through a 525/50 nm bandpass filter. Laser power, high voltage and offset were maintained constant. Brightfield images were obtained simultaneously. Over three independent replicates, images were made of a total of 43 and 31 worms from cultures treated with *frh-*

1(RNAi) and control vector (L4440), respectively. Quantification of mitochondrial density was done using Nikon's NIS-Elements imaging software. Images were randomized and analyzed blindly. 3D volume measurement was performed in four randomly placed 5 × 10 μm-wide rectangular ROIs. Mitochondrial density was expressed as the percentage of mitochondrial volume in the total analyzed volume.

Supplemental References

S1.   Simmer, F., Tijsterman, M., Parrish, S., Koushika, S.P., Nonet, M.L., Fire, A., Ahringer, J., and Plasterk, R.H. (2002). Loss of the putative RNA-directed RNA polymerase RRF-3 makes C. elegans hypersensitive to RNAi. Curr Biol *12*, 1317-1319.

S2.   Rea, S.L., Ventura, N., and Johnson, T.E. (2007). Relationship between mitochondrial electron transport chain dysfunction, development, and life extension in Caenorhabditis elegans. PLoS Biol *5*, e259.

S3.   Schiavi, A., Torgovnick, A., Kell, A., Megalou, E., Castelein, N., Guccini, I., Marzocchella, L., Gelino, S., Hansen, M., Malisan, F., et al. (2013). Autophagy induction extends lifespan and reduces lipid content in response to frataxin silencing in C. elegans. Exp Gerontol *48*, 191-201.

S4.   Trent, C., Tsuing, N., and Horvitz, H.R. (1983). Egg-laying defective mutants of the nematode Caenorhabditis elegans. Genetics *104*, 619-647.

S5.   Guccini, I., Serio, D., Condò, I., Rufini A, Tomassini, B., Mangiola, A., Maira, G., Anile, C., Fina, D., Pallone, F., et al. (2011). Frataxin participates to the hypoxia-induced response in tumors. Cell Death Dis *2011*.

S6.   Stiernagle, T. (2006). Maintenance of C. elegans. WormBook, 1-11.

S7.   Kamath, R.S., and Ahringer, J. (2003). Genome-wide RNAi screening in Caenorhabditis elegans. Methods *30*, 313-321.

S8.   Asikainen, S., Rudgalvyte, M., Heikkinen, L., Louhiranta, K., Lakso, M., Wong, G., and Nass, R. (2010). Global microRNA expression profiling of Caenorhabditis elegans Parkinson's disease models. Journal of molecular neuroscience : MN *41*, 210-218.

S9.   Springer, W., Hoppe, T., Schmidt, E., and Baumeister, R. (2005). A Caenorhabditis elegans Parkin mutant with altered solubility couples alpha-synuclein aggregation to proteotoxic stress. Hum Mol Genet *14*, 3407-3423.

S10. Samann, J., Hegermann, J., von Gromoff, E., Eimer, S., Baumeister, R., and Schmidt, E. (2009). Caenorhabditits elegans LRK-1 and PINK-1 act antagonistically in stress response and neurite outgrowth. J Biol Chem *284*, 16482-16491.

S11. Gourley, B.L., Parker, S.B., Jones, B.J., Zumbrennen, K.B., and Leibold, E.A. (2003). Cytosolic aconitase and ferritin are regulated by iron in Caenorhabditis elegans. J Biol Chem *278*, 3227-3234.

S12. Denzel, M.S., Storm, N.J., Gutschmidt, A., Baddi, R., Hinze, Y., Jarosch, E., Sommer, T., Hoppe, T., and Antebi, A. (2014). Hexosamine pathway metabolites enhance protein quality control and prolong life. Cell *156*, 1167-1178.

S13. Torgovnick, A., Schiavi, A., Testi, R., and Ventura, N. (2010). A role for p53 in mitochondrial stress response control of longevity in C. elegans. Exp Gerontol *45*, 550-557.

S14. Castelein, N., Hoogewijs, D., De Vreese, A., Braeckman, B.P., and Vanfleteren, J.R. (2008). Dietary restriction by growth in axenic medium induces discrete changes in the transcriptional output of genes involved in energy metabolism in Caenorhabditis elegans. Biotechnol J *3*, 803-812.

S15. Hoogewijs, D., Houthoofd, K., Matthijssens, F., Vandesompele, J., and Vanfleteren, J.R. (2008). Selection and validation of a set of reliable reference genes for quantitative sod gene expression analysis in C. elegans. BMC Mol Biol *9*, 9.

S16. Hellemans, J., Mortier, G., De Paepe, A., Speleman, F., and Vandesompele, J. (2007). qBase relative quantification framework and software for management and automated analysis of real-time quantitative PCR data. Genome Biol *8*, R19.

S17. Vandesompele, J., De Preter, K., Pattyn, F., Poppe, B., Van Roy, N., De Paepe, A., and Speleman, F. (2002). Accurate normalization of real-time quantitative RT-PCR data by geometric averaging of multiple internal control genes. Genome Biol *3*, RESEARCH0034.

S18. Williams, A., Sarkar, S., Cuddon, P., Ttofi, E.K., Saiki, S., Siddiqi, F.H., Jahreiss, L., Fleming, A., Pask, D., Goldsmith, P., et al. (2008). Novel targets for Huntington's disease in an mTOR-independent autophagy pathway. Nat Chem Biol *4*, 295-305.

S19. Gosai, S.J., Kwak, J.H., Luke, C.J., Long, O.S., King, D.E., Kovatch, K.J., Johnston, P.A., Shun, T.Y., Lazo, J.S., Perlmutter, D.H., et al. (2010). Automated high-content live animal drug screening using C. elegans expressing the aggregation prone serpin alpha1-antitrypsin Z. PLoS ONE *5*, e15460.

S20. Palikaras, K., Lionaki, E., and Tavernarakis, N. (2015). Coordination of mitophagy and mitochondrial biogenesis during ageing in C. elegans. Nature.

S21. Rosado, C.J., Mijaljica, D., Hatzinisiriou, I., Prescott, M., and Devenish, R.J. (2008). Rosella: a fluorescent pH-biosensor for reporting vacuolar turnover of cytosol and organelles in yeast. Autophagy *4*, 205-213.

S22. Mijaljica, D., Prescott, M., and Devenish, R.J. (2011). A fluorescence microscopy assay for monitoring mitophagy in the yeast Saccharomyces cerevisiae. Journal of visualized experiments : JoVE.

S23. Castelein, N., Muschol, M., Dhondt, I., Cai, H., De Vos, W.H., Dencher, N.A., and Braeckman, B.P. (2014). Mitochondrial efficiency is increased in axenically cultured Caenorhabditis elegans. Exp Gerontol *56*, 26-36.